Photoresist Derived Carbon Films as High Capacity Anodes for Lithium Ion Battery

M. Kakunuri[a], and C. S. Sharma[a]

[a] Department of Chemical Engineering, Indian Institute of Technology Hyderabad, Yeddumailaram, AP 502205, India

An epoxy-based negative photoresist (SU-8) was spin-coated on stainless steel (SS) wafers followed by two-step pyrolysis in inert atmosphere to yield dense carbon films to be used as anodes for lithium (Li) ion batteries. The selection of SS wafer substrates was in accordance with commercial Li ion battery architecture. Cyclic voltammograms confirm the passive layer formation by electrolyte decomposition in the initial cycle. Galvanostatic charge/discharge experiments in the range 0.01-3 V performed at a C-rate=0.1 C confirms the reversible intercalation of Li ions and shows higher gravimetric reversible capacity for these photoresist-derived carbon films on SS wafer substrates than graphite (400 mAh/g vs. 372 mAh/g for graphite). This high reversible capacity may be attributed to high disorder in photoresist derived-carbon as characterized by X-ray diffraction and Raman spectroscopy.

Introduction

Carbon is one of the anode materials most commonly used in commercial rechargeable lithium (Li) ion batteries. Depending on their crystalline structure and heat treatment, carbonaceous materials can be classified as graphite (highly crystalline), graphitizable soft carbons and non-graphitizable hard carbons (1). Among the various carbonaceous materials, graphite materials of different grade have been studied extensively with their reported Li ion intercalation capacities in the range of 215- 370 mAh/g which is closer to the theoretical capacity of graphite (372 mAh/g) (2-5). In contrast, hard carbons derived from various sources like epoxy novolac resins, phenolic resins, synthetic isotropic pitches, polymers and oxidized pitches show higher lithium insertion capacity (400-800 mAh/g) than that of graphite (6-9). Different mechanisms were proposed to explain the higher intercalation capacity of hard carbon materials; (i) adsorption of the Li ion on the internal surface of the nanopores formed by small graphene sheets arranged like a house of cards (6), (ii) trapping of a Li_2 covalent compound in between two benzene rings (10), and (iii) doping of Li at the edges and on the surface in small crystalline carbons apart from the Li insertion in between graphene layers with LiC_6 stoichiometry (11). Along with these crystalline imperfections surface functional groups (-OH, -COOH) and hydrogen contents which are very reactive to Li metal also play a significant role (12). However, the main disadvantage of using hard carbons as anode material for Li ion batteries is their higher irreversible capacity. This may be attributed to absorption of Li ions on the internal surface of nanopores formed by disordered single layer graphene sheets, reaction of Li with surface functional groups and electrode decomposition at

lower voltages around 0.5 V to form an ion conductive passivation film, known as a solid electrolyte interface (SEI).

The ability of photoresist polymers to fabricate three dimensional high aspect ratio structures provides an advantage over various other polymer precursors used in the literature (6,7,9) to prepare hard carbon anode materials. Using SU-8 (an epoxy negative phoresist) to form derived-carbon layers, Madou et al. fabricated high aspect ratio carbon posts that could be intercalated reversibly with Li ions (13-15). However, the reversible capacity for thin SU-8 derived-carbon films prepared on silicon wafer substrates was measured to be ~ 220 mAh/g (13-15) which was lower than that of graphite.

In this work, we consider the use of stainless steel (SS) wafer substrates to prepare thin SU-8 derived-carbon films. The selection of SS wafers as substrates is more apt as the same is used in the commercial Li ion battery. Various processing parameters such as pre- and post-baking conditions along with UV exposure dose were optimized to prepare smooth thin photoresist films on SS wafers by spin-coating. Later, two-step pyrolysis was done to ensure properly adhered and crack-free thin SU-8 derived-carbon films. Electrochemical tests (cyclic voltammetry and glavanostatic charge/discharge) were performed at C-rate = C/10 over the range 0.01-3 V.

Experimental

SU-8 2005 (Microchem Corp., MA) was spin-coated in a yellow room at 3000 rpm for 30 s on dehydrated single side polished SS substrates (MTI Corp., USA). After 10 min relaxation, films were soft-baked at 95 ^{0}C for 2 min. After cooling to room temperature films were exposed to UV light followed by post-exposure bake at 95 ^{0}C for 3 min to complete the crosslinking. The hard-bake of samples was carried out at 150 ^{0}C for 10 min.

As-prepared SU-8 films were then carbonized at 900 ^{0}C in the inert atmosphere using two-step pyrolysis in an alumina tube furnace (Nabertherm GmbH). Samples were introduced into the furnace at room temperature. The furnace tube was initially purged with 100 lph N_2 flow for 20 min. After initial purging, the N_2 flow rate was maintained constant at 30 lph. The furnace temperature was ramped up to 350 ^{0}C at 2 ^{0}C/min and samples were maintained at the same temperature for 20 min. These samples were further ramped up at 5 ^{0}C/min to 900 ^{0}C and held at 900 ^{0}C for 1 hour before cooling to room temperature in the presence of the inert gas atmosphere.

The prepared SU-8 derived-carbon films on SS wafers were then used as working electrodes and tested for their electrochemical performance using a galvanostat potentiostat (Biologic Potentiostat, Model: VSP). Lithium foil (99.9% pure, Sigma Aldrich) was used as counter electrode in a Swagelok cell assembly. 1 M solution of $LiPF_6$ in a 1:1 v/v mixture of ethylene carbonate and diethyl carbonate was used as an electrolyte while glass microfiber filters (Whatman Filters) were used as a separator. The Swagelok cell assembly was completely packed inside an argon-filled glove box with trace amounts of moisture and oxygen. The soaking time was maintained for 12 hours before galvanostatic cycling at a C-rate=C/10 to measure the Li ion intercalation capacity of SU-8 derived-carbon films as anode.

X-ray diffraction (XRD) patterns for photoresist-derived carbon films were obtained using a PANalytical X-ray diffractometer (Model: X'Pert PRO) with a CuKα radiation source, an accelerating voltage of 40 V and 30 mA current over a 2θ range from 10 to 80°. The Raman spectrum was recorded with a 532 nm laser using a Bruker Raman microscope spectrometer (Model: Senterra).

Results and Discussion

Preparation of smooth and crack free SU-8 derived carbon films on SS wafer

The thickness of spin-coated SU-8 photoresist films as measured with a 3D contact profiler (AEP Technology, USA) was found to be 5.2 ± 0.7 micron which was shrunk to 1.8 ± 0.4 micron by pyrolysis. Soft (pre-) baking conditions were optimized (at 95 °C for 90 s) to remove the solvent from the freshly coated photoresist films. The UV exposure dose was optimized to be 160 mJ/cm^2, 1.5 times larger than for photoresist films prepared on silicon wafers. A post-exposure bake was done at 95 °C for 3 min to complete the crosslinking of photoresist, similar to that for SU-8 films on silicon wafers. However, crosslinking of photoresist at high temperature generates internal residual stresses due to shrinkage. To reduce the possible cracks arising due to these residual stresses and to increase the adhesion of the films on the substrate, we introduced a hard-baking step for these photoresist films and optimized the conditions (150 °C for 10 min). Further pyrolysis conditions were also optimized and it was done in two steps as described in the experimental section. Two-step pyrolysis helps in releasing the internal stresses uniformly (14) and avoids cracking and thus peeling of the films from the substrate.

Structural characterization

Figure 1a and 1b show the XRD spectrum of a SS wafer and a thin SU-8 derived-carbon thin film on a SS wafer, respectively. The absence of the characteristic peak of the (0 0 2) plane at 2θ=26° suggests random stacking of graphene layers similar to a house of cards (Figure 1b). A sharp peak at 43° (Figure 1b) corresponds to (1 0 0) plane reflections without splitting into (1 0 0) and (1 0 1) that further indicates the absence of three dimensional arrangement (16, 17). Other peaks around 2θ = 45°, 63° and 74° (Figure 1a and b) corresponds to SS wafer reflections.

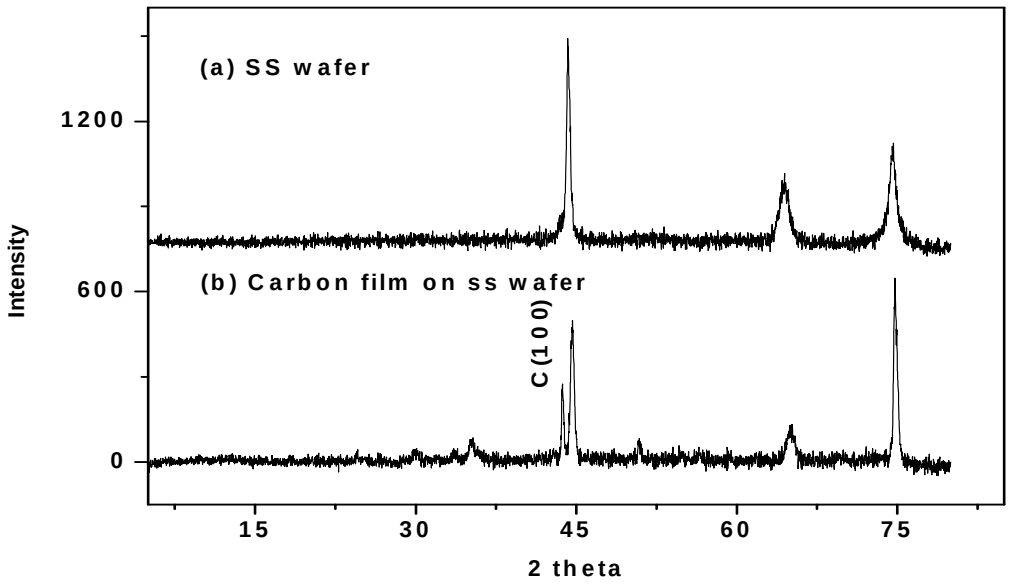

Figure 1: XRD spectrum of (a) only SS wafer; (b) SU-8 derived-carbon film on SS wafer.

Figure 2 shows the Raman spectrum for SU-8 derived-carbon films pyrolyzed at 900 °C. Peaks observed at 1336 nm^{-1} and 1596 nm^{-1} were associated with unorganized carbon scattering produced by imperfections (D band) and of in-plane motions of hexagonal network (G-band), respectively. The intensity ratio ($R = I_D/I_G$) of peaks corresponding to D and G bands, respectively was calculated to be 1.13. Additionally, the in-plane crystallite size (L_a) defined as the width of crystallite in the direction of graphite plane was also calculated to be 3.89 nm using the relation, $L_a = 4.4/R$ (18, 19).

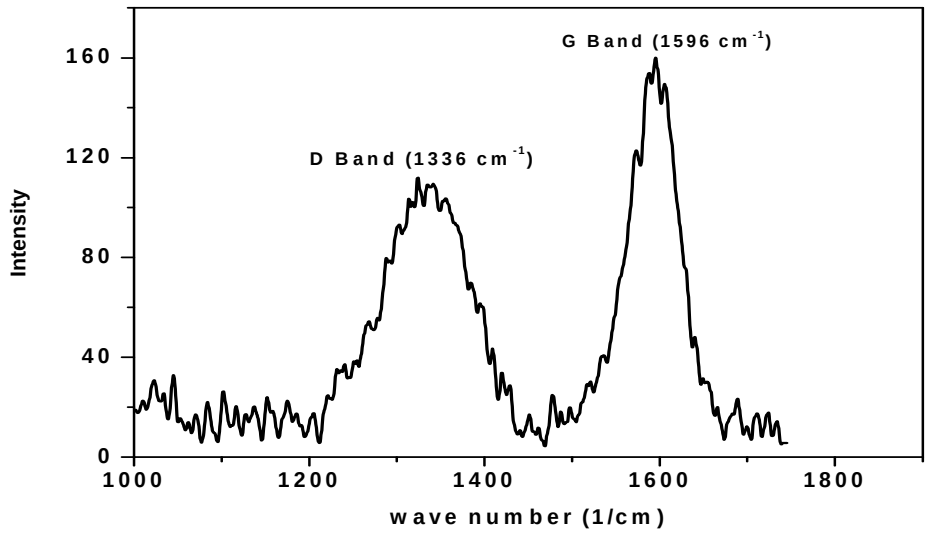

Figure 2: Raman spectrum of SU-8 derived-carbon film on SS wafer pyrolyzed at 900 ^{0}C.

XRD and Raman spectroscopy results clearly indicates that SU-8 derived carbon films contain randomly arranged graphene sheets as found in hard carbon materials.

Electrochemical characterization

Cyclic Voltammetry. The cyclic voltammogram shown in Figure 3 was recorded at 1 mV/s between 0 and 3 V. Higher current for the irreversible region in cycle 1 originated from passive layer formation on carbon films due to decomposition of electrolyte, absorption and intercalation of Li ions. However less current flow in the second and third cycles may be attributed to adsorption followed by intercalation of Li ions into the carbon film.

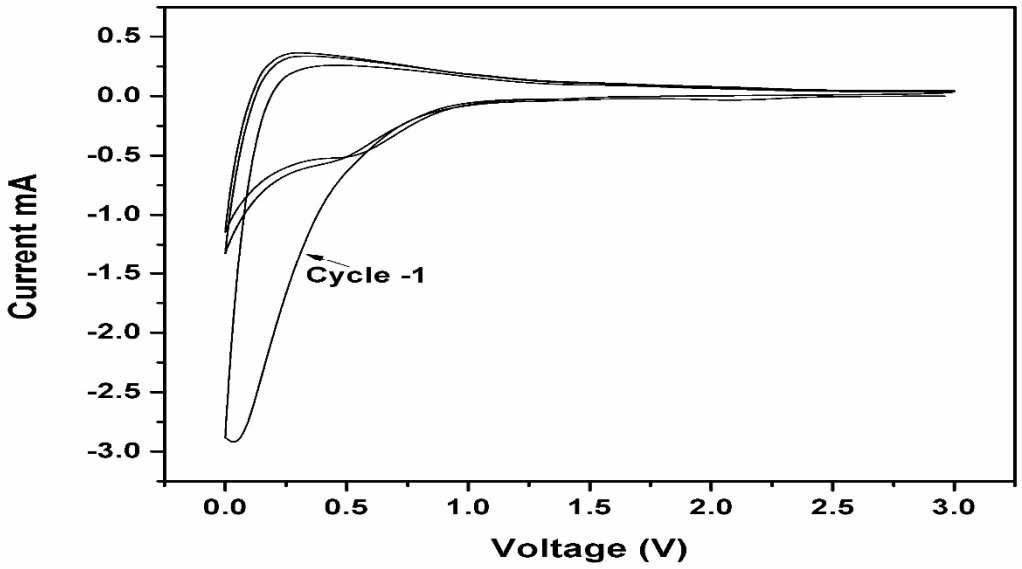

Figure 3: Cyclic voltammogram of SU-8 derived-carbon film on SS substrate.

Galvanostatic charge/discharge cycling: All glavanostatic charge/discharge experiments were carried out at room temperature with constant current corresponding to C-rate=0.1C for graphite. As shown in Figure 4, initial discharge capacity was very high compared to that for subsequent cycles. As discussed previously, this is due to electrolyte decomposition near to 0.4 V (6) and formation of a SEI layer. However after 20 cycles, gravimetric reversible capacity was found to be higher than that of the theoretical capacity of graphite (400 mAh/g vs. 372 mAh/g). Moreover, as compared to reported values of reversible capacity of SU-8 derived-carbon films (~220mAh/g) (14, 15) on silicon wafers, it was nearly double. The enhancement of reversible capacity may be attributed to a disordered structure in these carbon films similar to that for hard carbons and also possibly due to a lower resistivity of the SS wafer used as substrate. The coulombic efficiency as defined by the ratio of charge/discharge capacity was found to be more than 90% for any given cycle. The good cycling behavior of photoresist-derived carbon films and their high reversible capacity may be due to non-porous (dense) carbon films with no observable surface cracks and better adhesion with the substrate.

Electrochemical impedance spectroscopy (EIS): Impedance measurements shown in Figure 5 were done with a AC amplitude of 10 mV over the frequency range 10 mHz-100

KHz before and after 10 cycles of charge/discharge. The electrolyte resistance before and after cycling was found to be 1.43 Ω and 2.12 Ω, respectively. Similarly, the charge transfer resistance before and after cycling was found to be 17.1 Ω and 54 Ω, respectively. The increase in charge transfer resistance is due to formation of a passivation layer on the carbon film. These results further support the higher reversible capacity values obtained in this work compared to reported values (13-15) for SU-8 derived-carbon films on silicon wafers. For SU-8 derived-carbon films on silicon wafers, the charge transfer resistance after first charge was reported to be more than double (~45 Ω) (15). Additionally the electrolyte resistance was also more than one order of magnitude larger than shown in the present work.

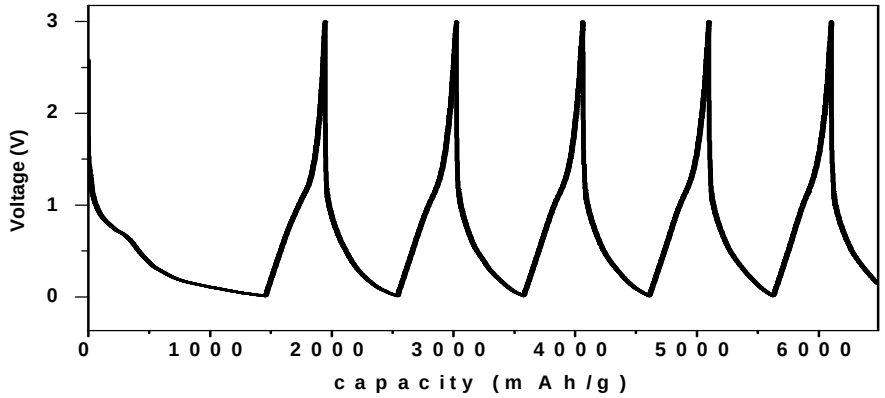

Figure 4: Galvanostatic charge-discharge curve for SU-8 derived-carbon films on SS substrate at 0.1 C-rate

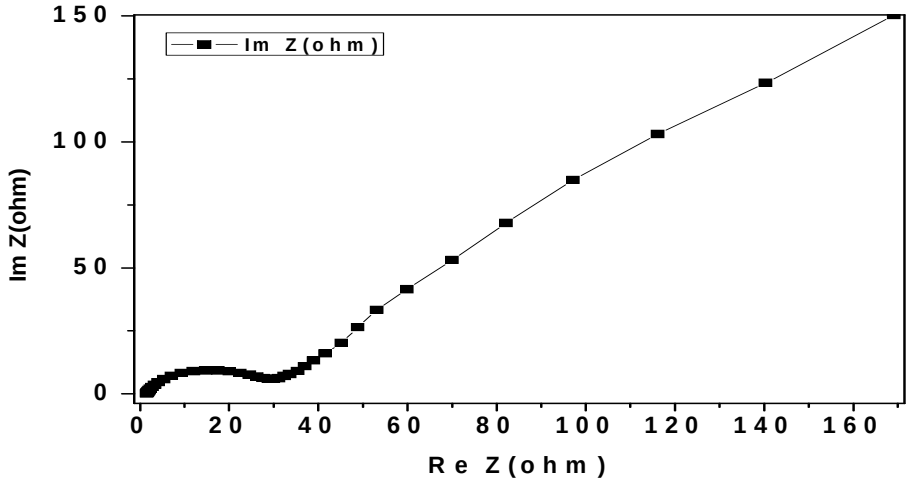

Figure 5: Electrochemical impedance spectroscopy results in the form of Nyquist plot for SU-8 derived-carbon film on SS wafer (a) before and (b) after 10 charge/discharge cycles.

Summary

An epoxy-based negative photoresist (SU-8) derived-carbon films were successfully prepared on SS wafer used as substrates and then further tested for their electrochemical performance as anode materials for Li ion battery. Galvanostatic charge/discharge

experiments showed higher reversible capacity (~400 mAh/g) as compared to that for graphite and earlier reported values, and showed improved coulombic efficiency. EIS measurements also supplement these findings. Structural characterization reveals that the disorder in these carbon films is similar to that for hard carbons. Higher capacity with enhanced coulombic efficiency make SU-8 photoresist-derived carbon films on SS wafers a better alternative for anode materials in Li ion batteries. Further patterning of these carbon films to yield 3-D carbon structures on SS substrates may be useful to further achieve the high energy density architecture for Lithium ion batteries.

Acknowledgments

Authors acknowledge the discussions with Prof. Marc Madou, University of California, Irvine. We also acknowledge Indian Institute of Technology Hyderabad for providing the required financial support to carry out this work.

References

1. R. E. Franklin, *Proc. R. Soc. Lond. A*, **209**, 196 (1951).
2. P. Ridgway, H. Zheng, A. F. Bello, X. Song, S. Xun, J. Chong and V. Battaglia, *J. Electrochem. Soc.*, **159**(5) A520 (2012).
3. H. Huang, W. Liu, X. Huang, L. Chen, E. M. Kelder and J. Schoonman, *Solid State Ionics*, **110**, 173 (1998).
4. H. Shi, J. Barker, M. Y. Saydi, R. Koksbang and L. Morris, *J. Power Sources*, **68**, 291 (1997).
5. K. Zaghib, G. Nadeau, K. Kinoshita, *J. Electrochem. Soc.*, **147**(6), 2110 (2000).
6. Y. Liu, J. S. Xue, T. Zheng and J. R. Dahn, *Carbon*, **34**, 193 (1996).
7. W. Xing, J. S. Xue, T. Zheng, A. Gibaud and J. R. Dahn, *J. Electrochem. Soc.*, **143**(11), 3482 (1996).
8. I. Mochida, C. Ku and Y. Korai, *Carbon*, **39**, 399 (2001).
9. A. Piotrowska, K. Kierzek, P. Rutkowski and J. Machnikowski, *J. Anal. Appl. Pyrolysis*, **102**, 1 (2013).
10. K. Sato, M. Noguchi, A. Demachi, N. Oki and M. Endo, *Science*, **264**, 556 (1994).
11. Y. Matsumura, S. Wang, T. Kasuh and T. Maeda, *Synth. Met.*, **71**, 1755 (2000).
12. T. Zheng, Y. Liu, E. W. Fuller, S. Tseng, U. V. Sacken and J. R. Dahn, *J. Electrochem. Soc.*, **142**(8), 2581 (1995).
13. C.Wang, G. Jia, L. H. Taherabadi and M. J. Madou, *J. MEMS*, **14**(2), 348 (2005).
14. C. Wang and M. Madou, *Biosens. Bioelectron.*, **20**, 2181 (2005).
15. G. T. Teixidor, R. B. Zaouk, B. Y. Park and M. Madou, *J. Power Sources*, **183**, 730 (2008).
16. S. Tzeng, *Carbon*, **44**, 1986 (2006).
17. J. M. Skowronski and K. Knofczynski, *J. New Mater. Electrochem. Syst.*, **9**, 359(2006).
18. F. Tuinstra and J. L. Koenig, *J. Chem. Phys.*, **53**(3), 1126 (1970).
19. F. J. Maldonado-Hodar, C. Moreno-Castilla, J. Rivera-Utrilla, Y. Hanzawa and Y. Yamada, *Langmuir*, **16**, 4367 (2000).